DEVELOPMENT OF A COMPUTER PROGRAM FOR PARAMETRIC SAILPLANE PERFORMANCE OPTIMIZATION

L.M.M. Boermans
Delft University of Technology

Presented at the XVIth OSTIV Congress
Chateauroux, France, 1978

SUMMARY

A computer program is presented for the analysis and synthesis of a sailplane speed-polar and subsequent calculation of cross-country performance in predefined meteorological conditions. Attention is focused on calculating the wing characteristics.

Wing induced drag, wing profile drag (including Reynolds number effects) and empennage drag are calculated. Either estimated miscellaneous drag data (i.e., fuselage drag, wing-fuselage interference drag, etc.) can be applied or data determined by analyzing the measured speedpolar of an existing sailplane.

For subsequent parametric studies, weight and/or wing parameters like span, aspect ratio, taper, twist or airfoil characteristics can be varied continuously. While the horizontal and vertical tailplane will be adjusted if necessary, the original miscellaneous drag area is taken constant at equal values of the lift coefficient.

If required, computer plots of the spanwise lift distribution and local lift coefficient at maximum wing lift coefficient (to assess stalling characteristics), the sailplane drag polar (in which wing drag contributions are shown) and the speedpolar are produced.

Cross-country performance is calculated assuming that optimum flight techniques are employed in given meteorological conditions. Depending on these conditions the highest possible cross-sountry speed, while maintaining average height, is realized by thermalling (with maximum rate of climb) or straight dolphin flying. The meteorological conditions are modeled as two regions with arbitrary constant vertical velocity of the air within each region - to be interpreted as spatial average values - and a thermal with specified vertical velocity profile.

If required, computer plots of cross-country speeds are generated for systematic variation of meteorological conditions (fixed sailplane configuration) or weight and aspect ratio (fixed meteorological conditions).

Some capabilities of the program are illustrated, starting from the measured speedpolar of the Astir CS.

1. INTRODUCTION

The computer program, written in Fortran IV, consists of a main program, 16 subroutines and 6 plotroutines. Following the schematic diagram of major functions of the program, Fig. 1, a review of methods and basic considerations will be presented and illustrated by some calculation results.

2. SPEEDPOLAR

In order to see the effect of parasitic drag differences on the speedpolar, it is interesting to compare two pairs of sailplanes: the ASW-15 vs. the ASW-19, and the Club Libelle vs. the Hornet. Each pair have aerodynamically the same wings, but differ in wing placement, landing gear configuration, fuselage/tailplane configuration, and forward fuselage shape. The speedpolars of the two pairs have been converted to similar weight and are shown in Fig. 2. While tailplane drag can be estimated, using measured airfoil data and some theory,no really good method is known to calculate the effects of wing-fuselage interference. The calculation of the drag of real fuselage shapes, trim and separated flow is also problematic.

In order to study the effects of changing the wing and weight of a particular sailplane, the computer program is arranged such that realistic miscellaneous drag data (i.e., parasitic drag less empennage drag), determined by analyzing the measured speedpolar of that sailplane first, can be taken into account. However, apart from this special feature, estimated miscellaneous drag area

data can be used as input data.

Following the former procedure for present purposes, the Astir CS has been chosen as the initial sailplane, mainly because some remarkable aspects (new airfoil, low aspect ratio) have been incorporated in this commercially succesful sailplane. Moreover, with respect to the measured speedpolar, it is noticed in Ref. 2 : "Die Anzahl und die geringe Streuung der Messpunkte ergeben nun eine eindeutige Polare."

Fig. 3 shows the input data taken from the measured speedpolar, except for the data beyond 180 km/h. In order to estimate this unmeasured high speed part of the polar, needed for the parametric studies which will be described, an extrapolated constant parasitic drag coefficient was assumed, as shown in Fig. 7 in terms of drag area. Supplemented with calculated wing drag coefficients, the missing speedpolar data was obtained.

The curve, fitted to the data by a least squares method, is given by the relationship found by Eppler (Ref. 3)

$$C = \sum_{k=1}^{N} A_k \, (v - 0.9\, V_{min})^{4-k}$$

where

A_k = constants

C = rate of sink, negative, m/s

V = forward speed, m/s

Most satisfactory results are obtained for $k = 9$.

When analysing (or synthesizing) a sailplane speedpolar, wing data, empennage data, weight and aerodynamic characteristics of the airfoils - two at most - are inputs to the program. The drag characteristics of the airfoils are tabulated as a function of lift coefficient and Reynolds number, and a computer plot can be produced to check the input data. Fig. 4 shows the measured data (Laminar Wind Tunnel of the University of Stuttgart) of the 19.2% thick airfoil E603 applied in the Astir CS wing. Calculation of spanwise lift distribution is based on the semi-empirical lifting line method by Diederich (Ref. 4), and the induced drag is calculated using the well known method of Sivells and Neely (Ref. 5). In order to assess stalling characteristics, the local lift coefficient at maximum wing lift coefficient - defined as the wing lift coefficient for which the local section lift coefficient at any position along the span is equal to the local maximum lift coefficient for the corresponding section - is calculated in an iterative way because the local maximum lift coefficinet depends on Reynolds number. Moreover, when linear lofting is applied between fairing stations with different airfoil thickness ratio, the local maximum lift coefficient for intermediate wing sections is estimated from the maximum lift coefficients of the given airfoils at local Reynolds number, assuming a linear variation of maximum lift coefficient with local thickness. Fig. 5 shows the results for the untwisted Astir wing.

It is found that the calculated maximum wing lift coefficient is close to the value calculated from the minimum measured polar speed, at least for the cases considered till now. In the case of the Astir CS these values are, for instance, 1.29 and 1.30 respectively.

With regard to stall progression, the small margin at the aileron (Fig. 5) might lead to the conclusion that the Astir CS would show bad stalling characteristics. However, this type of plot does not show the overriding influence on airplane stall behaviour of the E603 characteristics beyond maximum lift coefficient. In designing this airfoil, special care was taken to assure good stalling characteristics (Ref. 6); measurements indeed show an almost maximum lift coefficient over some 10 degrees of attack. In addition, drag increase beyond stall is probably moderate.

Wing profile drag is obtained, on the basis of strip theory, from the tabular two-demensional profile drag data. For interpolation or extrapolation with respect to this data, the profile drag coefficient at a given (local) lift coefficient is assumed to be linear in Re^{-1}. Again, when linear lofting is applied, the drag coefficient of intermediate airfoil sections is estimated in the way described before.

For estimating the profile drag of the horizontal and vertical tailplane (thickness ratio usually .12 to .15), an approximating relationship, deduced from measured minimum drag data of symmetrical airfoils (Ref. 7) is used:

$$10^3 \, C_{d_p} = 3 + 10 \, \frac{t}{c} + \frac{20 \, \frac{t}{c}}{10^{-6} \, Re_{\bar{c}}}$$

where

$\frac{t}{c}$ = thickness ratio

The induced drag contribution of the

horizontal tailplane, which is very small, is also taken into account in a simple way.

Fig. 6 gives the sailplane drag polar, calculated from the Astir CS speedpolar, in which the wing induced drag, wing profile drag and parasitic drag contributions are shown. As always, the wing gives the largest contribution to the total drag. The increase in profile drag when the wing is operating beyond the low-drag bucket, is clearly indicated. Next step in the program is curve-fitting of the speedpolar (again), where minimum flight speed is determined from the calculated maximum lift coefficient in order to get a consistent basis for comparison when changing weight or wing parameters. The speedpolar close to minimum flight speed is adjusted by suitable extrapolation. A plot can be produced (used in Fig. 10, 11, 12 and A1).

Frequently the parasitic drag area, Fig. 7, is taken constant at all values of C_L considered. However, this may lead to an unsatisfactory prediction of the speedpolar as shown in Fig. 8, assuming a typical value of .05 m^2 for instance. In an attempt to take more realistic data into account when changing weight or wing parameters (next step), the original miscellaneous drag area is taken constant at equal values of the lift coefficient, while the drag contributions of the horizontal and vertical tailplane, adjusted if necessary, are calculated.

Adjustment of the vertical and horizontal tailplane is based at present on the assumption that tail volume ratio of the Astir CS remain unchanged, which seems plausible from Fig. 9. Data of the Standard Class sailplanes (aspect ratio varies from 17.2 to 26.4) are determined by using the relation:

$$\text{lift curve slope} = \frac{2\pi \text{ A.R.}}{\text{A.R.} + K}$$

$K = 2$ for high A.R.

3.15 for low A.R.

and assuming a 15% increase in lift gradient of the vertical tailplane when a T-tail is applied. Tailplane aspect ratio of these sailplanes (except for Phoebus B1 and Mistral) do not vary much, so in adopting aspect ration of the Astir CS tailplanes adjustment simply means

$$\frac{S_v}{S} = \text{constant} \qquad \frac{S_h}{S} = \frac{\text{constant}}{\text{A.R.} + 2}$$

where the constants are calculated from Astir CS data.

Tailplane profile drag and induced drag are calculated then in the way described before.

Changing wing parameters and weight can be done continously and each of the preceding plots can be generated, if required.

2.1. ILLUSTRATIVE CALCULATION RESULTS

Fig. 10 and 11 present some results concerning the effect of airfoil selection on the speedpolar of the Astir CS, using data of some typical airfoils, all measured in the same wind tunnel (Ref. 7), thus being suitable for comparison purposes. Nevertheless, the results should be interpreted with care, considering the differences in characteristics of a particular airfoil when measured in different wind tunnels, together with possible differences in airfoil contour between wind tunnel models and actual wing application (Ref. 7,8,9 and 10).

Except for the application of FX61-184 which shows a nearly constant maximum lift coefficient during the stall similar to E603, a linear lofted geometric twist of 2 degrees at the tip was applied to assure acceptable stalling characteristics.

Application of FX61-184 results in an improved speedpolar; best glide ratio increases about 1.5 point. With FX66-17A11-182 the minimum flight speed is decreased, while the polar is equal to the Astir CS polar between 75 and 110 km/h; however, beyond 110 km/h the speedpolar considerably deteriorates. Application of FX61-184 for the inner wing, and linear lofting the outer wing to FX60-126 at the tip, results in a speedpolar which does not deviate significantly from the single FX61-184 case below about 120 km/h. At higher speeds up to 200 km/h the polar approximates the polar of the Astir CS. Finally, from the speedpolar calculated for the combination of FX61-163 and FX60-126 it is noticed that a thinner wing does not necessarily lead to a better polar.

Fig. 12 illustrates some typical alterations of the Astir CS speedpolar when weight and aspect ratio (not the span) are changed, taking some practical figures into account. The speedpolar of the Astir CS is calculated for a wing loading of 28.2 kgf/m^2 (empty weight plu 90 kgf) and 32.8 kgf/m^2 (extra weight of 57 kgf). The latter wing loading corresponds to the wing loading at empty weight plus 90 kgf of the LS-1f, which has the highest aspect ratio of high performance German production type Standard Class sailplanes nowadays: 23.1 Except for the Phoebus

A/B, the Astir CS has the lowest one. After changing the aspect ratio of the Astir CS wing into 23.1 - which means a decrease of 21% in wing surface and hence in wing chord - and adjusting the tailplanes, the speedpolars are calculated for wing loadings of 32.8 kgf/m^2 and 38.7 kgf/m^2 (similar extra weight of 57 kgf). At wing loading 32.8 kgf/m^2 the speedpolar of the high aspect ratio configuration differs from the speedpolar of the Astir CS as a result of an increased wing profile drag (due to lower Reynolds number), an increased miscellaneous drag coefficient, and a decreased induced drag coefficient, all at equal values of the lift coefficient or forward speed. Total wing drag coefficients are almost equal at speeds higher than 130 km/h thus evidently the higher miscellaneous drag coefficient for the high aspect ratio sailplane is the reason for the increased rate of sink there. Total drag coefficients are equal at 109 km/h, and at lower speeds the decrease of the induced drag coefficient for the high aspect ratio wing is more than the increase of miscellaneous and wing profile drag coefficient together, resulting in a better low speed part of the polar. Minimum flight speed is hardly changed.

In addition, wing loading greatly affects the speedpolar, as indicated in the figures. For instance, the lower possible wing loading of the Astir CS results in a lower minimum flight speed and certainly better climbing performance than those of the high aspect ratio version at the lower weight; however, at speeds higher than 85 km/h (already) the speedpolar of the latter configuration is clearly superior. Because cross-country performance depends on both climbing and straight flight performance, it is clear that only a detailed study can give an answer to the question of what aspect ratio is optimal at relevant meteorological conditions, considering practical minimum weight and the use of water ballast. Results of such studies, Ref. 3, 6, 11, and 12 indicate that for a Standard Class sailplane an aspect ratio of 15-20, i.e., lower than the aspect ratio of most of the current high performance Standard Class sailplanes, should be the best compromise. Therefore, and because of the application of a new airfoil and the availability of a good polar, the Astir CS was an interesting case to illustrate some capabilities of the program.

Present results clearly indicate the importance of proper airfoil design or selection in combination with aspect ratio and weight; however, it is beyond dispute that many other aspects, such as intended use, cost, structure, aerodynamics of parts other than the wing (Fig. 2), have to be considered carefully as well when designing a sailplane with desired characteristics.

3. CROSS-COUNTRY PERFORMANCE

Cross-country performance is calculated assuming that optimum flight techniques are employed in given meteorological conditions. These conditions are modeled as two regions with arbitrary constant vertical velocity of the air within each region, to be interpreted as spatial average values (see Appendix), and a thermal with specified updraft velocity distribution. The ratio of the distance with the (highest) upward constant velocity of the air (or the lowest downward constant velocity of the air) to the entire range is specified, while the extent of the thermal is not taken into account separately.

Depending on the purpose of investigation or the interpretation of the meteorological model, climbing performance when circling in the thermal or in a region with constant upward velocity of the air (optional in the program) can be taken into account. When both modes are permitted, the program selects the best rate of climb.

The updraft velocity distribution of the thermal is assumed to be of axial symmetry (as statistically may be the case; Ref. 13 and Ref. 14 type B thermal), and circling in it takes place at that radius, i.e., at that combination of speed and angle of bank which gives maximum rate of climb. As elucidated in Ref. 15, the criterion for obtaining minimum sink rate at any radius of turn, expressed in terms of the speedpolar (being the datum for performance calculations), is:

$$\tan^2 \psi = \frac{-\frac{dC}{dV}}{3\frac{C}{V}}$$

With this relation and with

$$V_c = \frac{V}{\sqrt{\cos \psi}}, \quad C_c = \frac{C}{\sqrt{\cos^3 \psi}}, \quad R = \frac{V^2}{g \sin \psi}$$

and the given thermal updraft velocity distribution, maximum rate of climb can be calculated in an iterative way.

Here

g = acceleration of gravity, m/sec^2

R = radius of turn, m

ψ = angle of bank, degrees

and subscript c denotes circling conditions.

When circling in an updraft region with constant air velocity, climbing performance is calculated for a specified angle of bank, applying the same flight technique.

The optimum speed-to-fly in glide penetration through the regions with constant (average) vertical velocity of the air, is calculated from the equation upon which the MacCready Ring and the well-known graphical construction are based:

$$V = \frac{C + W - RS}{\frac{dC}{dV}}$$

where

W = local vertical velocity of the air, positive upwards, m/sec

RS = zero-setting of the MacCready ring, m/sec

For calculating and comparing maximum cross-country speeds, the usual assumptions are made that average height is maintained and that the flight is not hindered by proximity to cloud base or ground. Under these conditions (and without going into theoretical detail), the following modes of cross-country flying appear to be relevant, depending on sailplane performance and meteorological conditions:

- thermalling, i.e., flying straight according to the command of the MacCready Ring (dolphining) through the regions with constant (average) vertical velocity of the air, and gaining altitude by circling in the specified updraft. The zero-setting of the ring is in accordance with the rate of climb achieved by circling.
- straight dolphining, i.e., just flying straight through the regions above-mentioned according to the command of the MacCready Ring, set at the appropriate value. This value, being dependent on the overall distribution of vertical air velocity, is found in an iterative way.

When both modes are possible, the program selects the one giving the highest cross-country speed, achieved at the highest zero-setting of the ring.

Finally, in aid of parametric studies, some computer plots of cross-country performance can be generated for systematic variation of meteorological conditions, weight and aspect ratio as specified in Fig. 1. Only two illustrative examples will be discussed here.

3.1 ILLUSTRATIVE CALCULATION RESULTS

In order to show the maximum cross-country speeds at the different modes and accompanying interpretations in one figure, Fig. 13 was generated. Considering the part of the figure above the horizontal broken line first, the Astir CS is flown through air which has a vertical velocity W_1 (vertical axis) over part of the flight path (beta), while $W_2 = 0$ elsewhere.

As stated in the Appendix, W_1 and W_2 can be interpreted as average values provided that the vertical velocity of the air does not vary too much. When circling with an angle of bank of, say, 40 degrees the rate of climb will be (at least) equal to W_1 minus the rate of sink of the sailplane (1.15 m/s). Cross-country speeds at the circumstances on left side of the oblique broken line are obtained by climbing that way in order to maintain average height, while straight dolphining is practiced in the remaining circumstances. At beta = 1 the flight is horizontal (on an average) and the cross-country speed corresponds to the polar flight speed for which $-C = W_1$. The result for beta = 0, making the picture complete, should be interpreted as a climb in extremely localized areas with strength W_1, while $W_2 = 0$ over (practically) the entire flight path.

In the lower part of the figure an additionally specified thermal, in which a rate of climb 0.80 m/s is achieved, determines the cross-country speeds on the left side of the dotted line. On the right side of this line the thermal is ignored because the combinations of W_1, W_2 and beta permit straight dophin flying.

Fig. 14 shows the effect of weight on the cross-country speed of the Astir CS, penetrating through still air (on an average) and climbing in thermals having a linear distribution of vertical velocity in the radius of turn region of interest (Ref. 12). While the extrapolated (!) thermal velocity in the center Wth_{max} is varying, the gradient remains constant.

For 12 sailplanes the gradient of the radius of turn versus rate of sink curve was plotted against the corresponding angle of bank, assuming flight techniques which result in minimum rate of sink at any radius of turn respectively any angle of bank. Average

values of these gradients are .005 $m/s/_m$ and .027 $m/s/_m$ at an angle of bank 30 degrees and 45 degrees respectively. These values are close to the average of the values proposed in Ref. 12 representing wide and narrow thermals respectively. (Besides, the value .015 $m/s/_m$ for an angle of bank 40 degrees, as proposed in Ref. 16, corresponds to the average of the gradients obtained at that angle of bank.

The oblique line in Fig. 14 shows the optimum weight when climbing in thermals with gradient .027 $m/s/_m$. A similar figure was generated for thermals with gradient .005 $m/s/_m$ and values between parentheses in the following are valid for this gradient.

Assuming a weight without water ballast of 350 kgf as before, the Astir CS has to be flown unballasted in thermals having a Wthmax below 5.5 m/s (2.6 m/s), thus attaining a rate of climb below 2.8 m/s (1.3 m/s) as indicated in Fig. 14. When the thermal is only 0.9 m/s (0.5 m/s) stronger, the Astir CS has to be flown already (!) with full water tanks (90 liter), attaining a rate of climb 3.2 m/s (1.6 m/s). Corresponding cross-country speeds are 92 km/h (66 km/h) at 350 kgf and 104 km/h (76 km/h) at 440 kgf. When flying the full ballasted sailplane, all water should be drained when a rate of climb 2.3 m/s (1.1 m/s) can not be realized.

Considering permissable weights without ballast and with 90 kgf water ballast, and the corresponding angles of bank when climbing, the following practical numbers appear worth remembering when flying the Astir CS with full water tanks under the conditions mentioned and not taking tactical considerationd into account. Depending on the angle of bank when climbing, all water should be drained when the rate of climb does not exceed 2.25 m/s at an angle of bank of 45 degrees, going down to 1 m/s at an angle of bank of 30 degrees.

4. FINAL REMARKS

The author is indebted to (in alphabetic order) L. van Rijn, H.L.J. Schunselaar, D.J. Spiekhout and W.J. Tuil, all students at the time, for their contributions and pleasant cooperation in developing the present computer program.

Extension of this program is focused on the application of flaps and reliable estimation of fuselage drag and wing-fuselage interference effects.

It is hoped that in the end a program will be available for parametric performance optimization of a complete sailplane.

REFERENCES

1. Laurson, H. and Zacher, H.,"Flugmessungen mit 25 Segelflugzeugen," *Aero-Revue 10, 11, 12*, 1973.

2. Laurson, H. and Zacher, H., "Flugmessungen an 35 Segelflugzeugen und Motorseglern," *Aerokurier 2,3,4,5*, 1977/

3. Eppler, R., "When Should We Use Water Ballast?," NASA CR-2315, 1972.

4. Diederich, F.W., "A Simple Approximate Method for Calculating Span Wise Lift Distributions and Aerodynamic Influence Coefficients at Subsonic Speeds," NACA TN 2751, 1952.

5. Sivells, J.C. and Neely, R.H., "Method of Calculating Wing Characteristics by Lifting-line Theory Using Nonlinear Section Lift Data," NACA TN 1269, 1947.

6. Eppler, R., "Die Optimale Auslegung und Profilierung eines 15-m Segelflugzeugs ohne Wölbklappen," *Aerokurier 4*, 1976.

7. Althaus, D., "Stuttgarter Profilkatalog I," Institut für Aerodynanik und Gasdynamik der Universität Stuttgart, 1972.

8. Boermans, L.M.M. and Blom, J.J.H., "Low Speed Aerodynamic Characteristics of an 18% Thick Airfoil Section Designed for the All-flying Tailplane of the M-300 Sailplane," Delft University of Technology, Report LR-226, 1976.

9. Gooden, J.H.M., "Experimental Low Speed Aerodynamic Characteristics of the Wortmann FX66-S-196 V1 Airfoil," OSTIV Congress, 1978, Chateauroux, France.

10. Somers, D.M., "Experimental and Theoretical Investigation of Differences Between a Manufactured and the Corresponding Design Airfoil Section," *Technical Soaring, Vol. IV, No. 2*, 1976.

11. Irving, F.G., "Computer Analysis of the Performance of 15-m Sailpalnes," NASA CR-2315, 1972.

12. Horstmann, K.H., "Neue Modellaufwindverteilungen und ihr Einfluss auf die Auslegung von Segelflugzeugen," *Aero Revue 3*, 1977.

13. Chernov, V.V., "Results of Research in the Field of Structural Strength Limits for Sporting Gliders," *OSTIV publication VIII.*

14. Konovalov, D.A., "On the Structure of Thermals," *OSTIV publication XI.*

15. Eppler, R., "Der Genstigste Kreisflug von Segelflugzeugen," *Zeitschrift fur Flugwissenschaften, Heft 1*, 1954.

16. Waibel, G., "Gedanken uber Sinn und Moglichkeiten des Wasserballastes bei Standardklassen-Segleflugzeugen," *Aerokurier 6*, 1973.

17. Milford, J.R.,"Some Thermal Sections Shown by an Instrumented Glider," *OSTIV publication XII.*

APPENDIX A

When flying straight and according to the command of the MacCready Ring through a region with arbitrary vertical velocity distribution of the air, the resulting mean forward speed of the sailplane is:

$$\bar{V} = \frac{1}{\int_0^1 \frac{1}{V} d(x/L)} \qquad (1)$$

where

x = distance along flight path, m

L = total distance, m

The instantaneous forward speed of the sailplane V is determined by the well-known equation for (quasi-) stationary flight conditions:

$$V = \frac{C + W - RS}{\frac{dC}{dV}} \qquad (2)$$

where

C = instantaneous rate of sink (negative), m/sec

W = local vertical velocity of the air (positive upwards), m/sec

RS = zero setting of the MacCready Ring, m/sec

The spatial average of W is given by:

$$\bar{W} = \int_0^1 W \, d(x/L) \qquad (3)$$

It can be shown that $\bar{V}$ is found directly at $\bar{W}$ for any value of RS by using (2) when the relationship between C and V (polar) is

$$C = K_3 V - (K_1 - RS) - \frac{K_2}{2V} \qquad (4)$$

This is the result of simply assuming a linear relationship betwen W and 1/V (considering (1) and (3):

$$W = K_1 + K_2 \frac{1}{V} \qquad (5)$$

and, substituted into (2), solving the resulting differential equation. Moreover

$$\frac{H}{L} = \int_0^1 \frac{C + W}{V} \, d(x/L) \qquad (6)$$

where

H = change of height

and, from (4) and (5)

$$\frac{C + W}{V} = K_3 + \frac{K_1}{K_2}\left(\frac{K_1}{2} - RS\right) + W\left(\frac{RS - K_1}{K_2}\right) + \frac{W^2}{2K_2} \qquad (7)$$

Without going into further detail, it appears that relevant parts of the speedpolar can be approximated very well by (4) regardless of the zero setting of the ring, provided that W does not vary too much, say less than 2 m/s (depending on the degree of accuracy one requires). As an example, Fig. A1 shows such an approximation, simply obtained by inserting three points of the polar (marked by a cross) into (4) in order to determine the constants K_1, K_2 and K_3. In this case, the Astir CS is flown straight and according to the command of the MacCready Ring (equation 2) at a zero setting of 1.6 m/s, through a region where W varies between -.25 m/s and 1.7 m/s. (These values are related to a measured vertical velocity distribution of the air over 2150 m followed by a thermal (Ref. 17, Fig. 4) in which a maximum rate of climb of 1.6 m/s could be obtained.)

The relevant part of the speedpolar to approximate is between 92 and 104 km/h, and values obtained are

$$K_1 = -3.681 \quad K_2 = 141.223 \quad K_3 = -.12760$$

when V and C are expressed in m/s. Moreover, investigation shows that $\frac{C + W}{V}$ according to (7) is always nearly proportional to W for the range of interest. Consequently $\frac{H}{L}$, or H when L is known (thus the time needed to climb to a specific height) can be found as well, approximately, at $\bar{W}$ for any value of RS, using relation (2).

Summarizing, for estimating cross-country performance, the spatial average of W may be taken, provided that the vertical velocity of the air does not vary too much and (quasi-) stationary flight conditions are fulfilled.

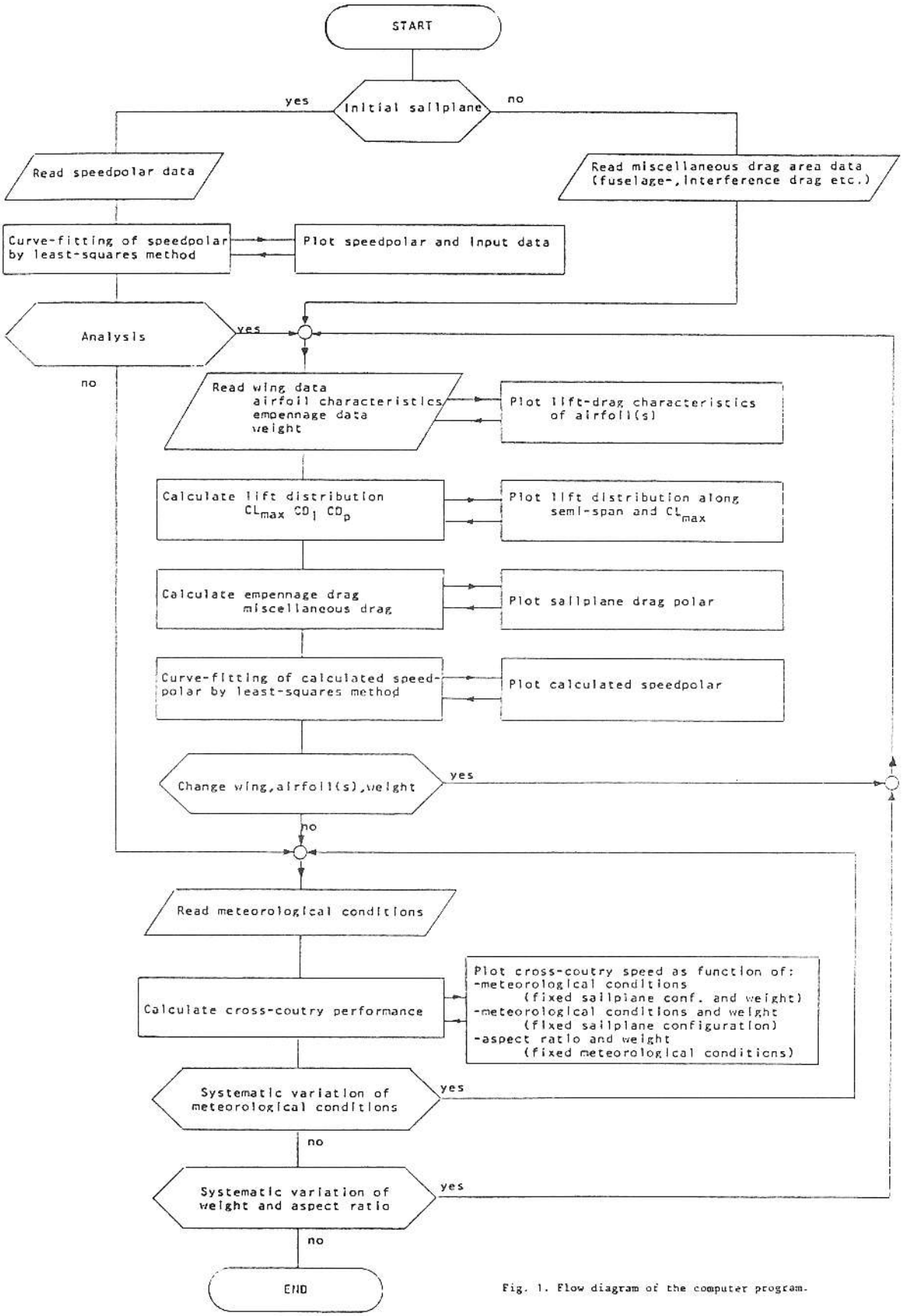

Fig. 1. Flow diagram of the computer program.

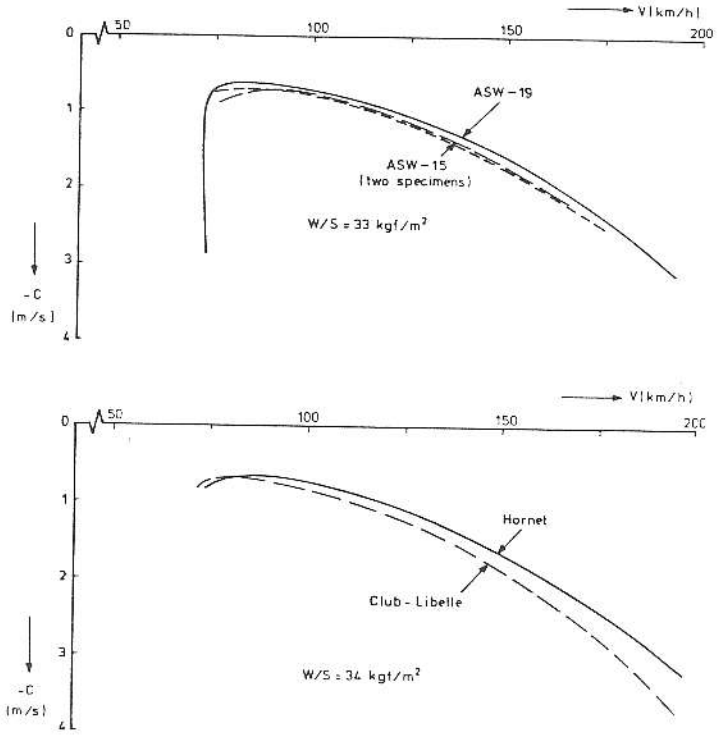

Fig. 2. Effect of parasitic drag; sailplanes (span 15 m.) have aerodynamically the same wing two by two.

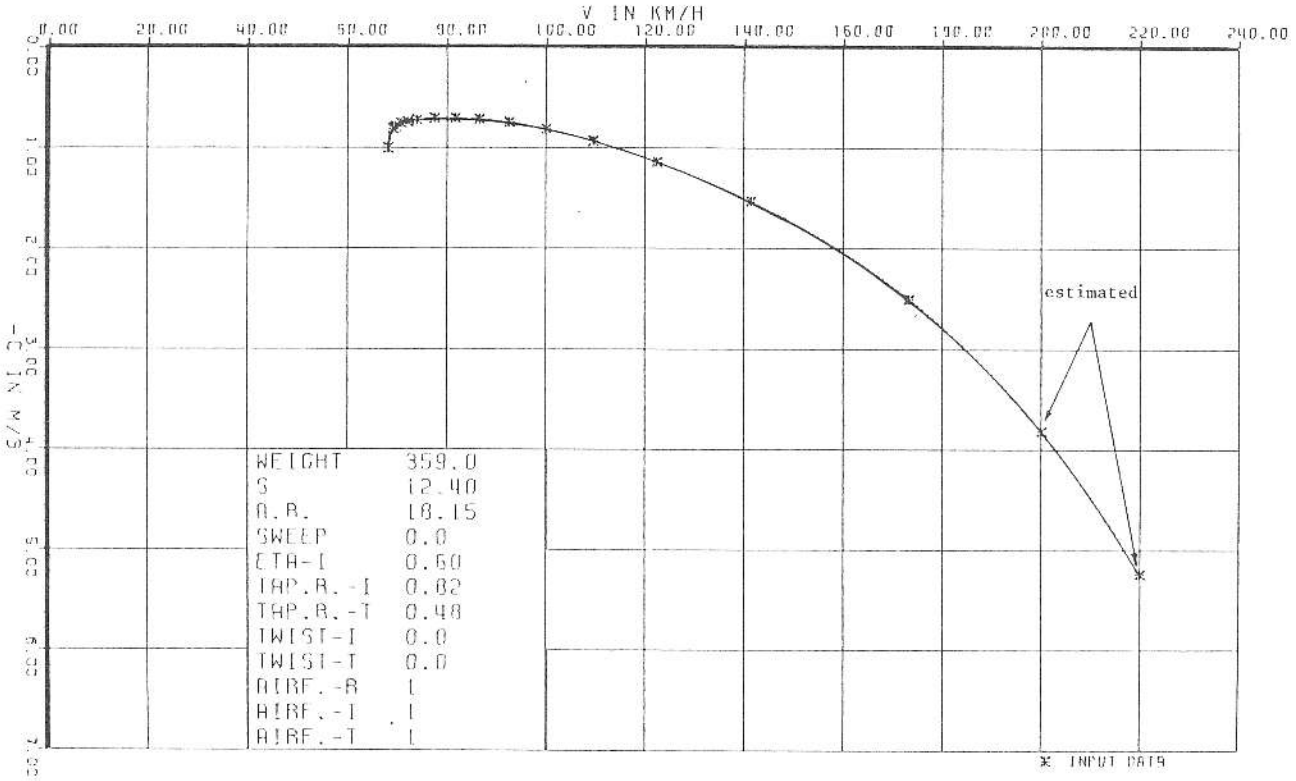

Fig. 3. Speedpolar of the Astir CS at weight 359 kgf. Input data taken from measurements (ref. 2) and estimated.

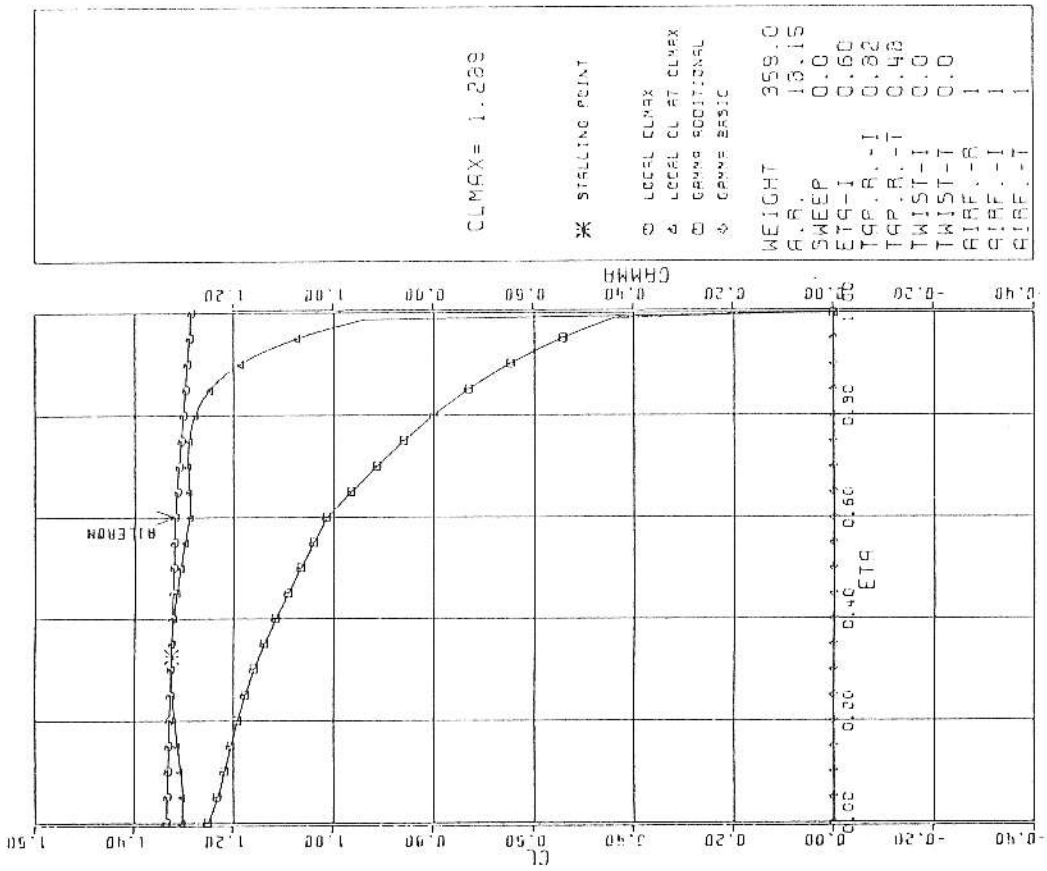

Fig. 5. Lift distribution (gamma) at wing lift coefficient 1.0, local lift coefficient and local maximum lift coefficient at maximum wing lift coefficient. Untwisted Astir CS wing.

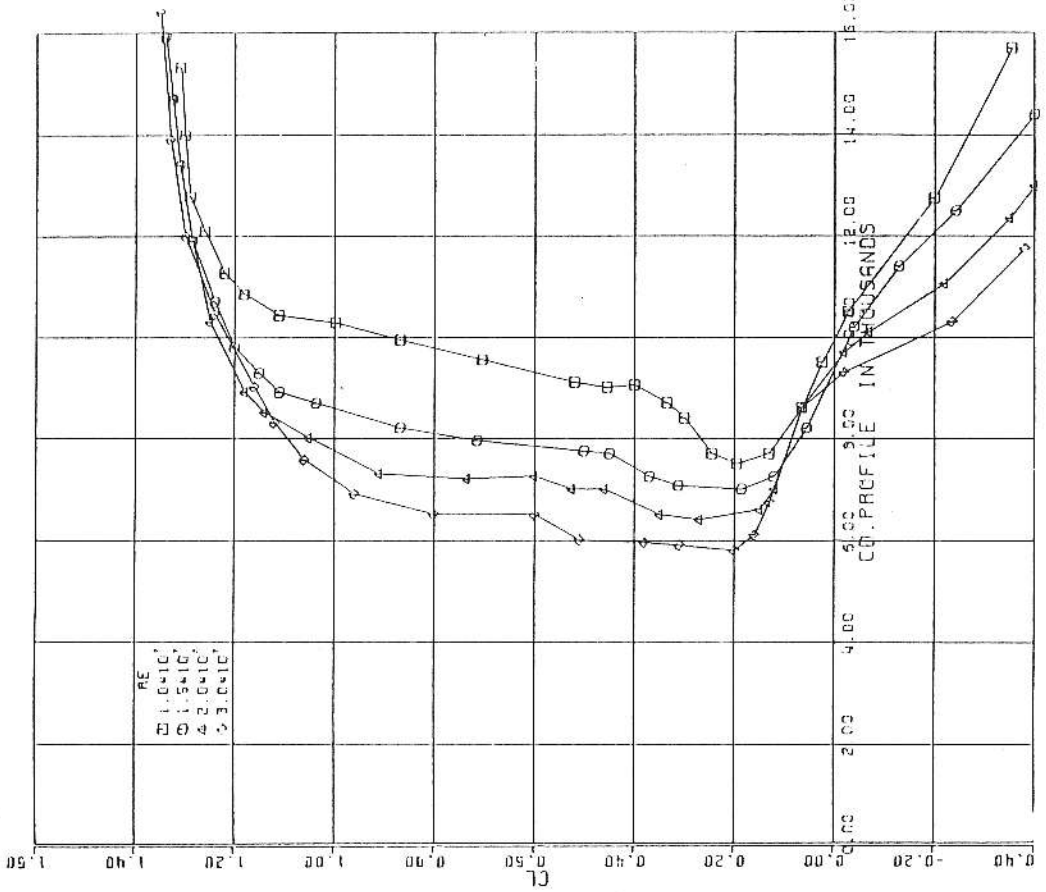

Fig. 4. Drag-characteristics of airfoil E603, applied in the Astir CS wing. Measurements: Laminar Windtunnel of the University of Stuttgart.

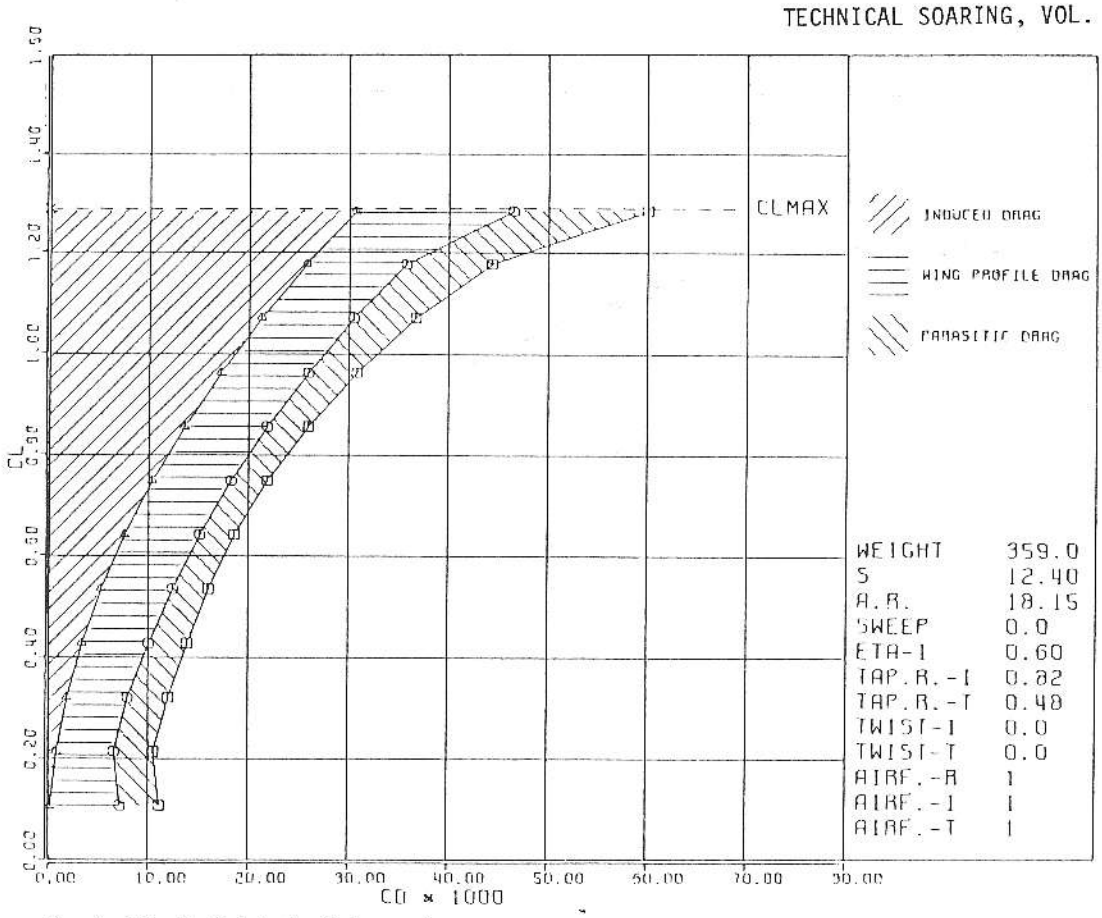

Fig. 6. Sub-divided Astir CS drag polar.

$$C_D = C_{D_P} + C_{D_I} + \left(\frac{\Sigma C_{D_S} S_S}{S}\right)$$

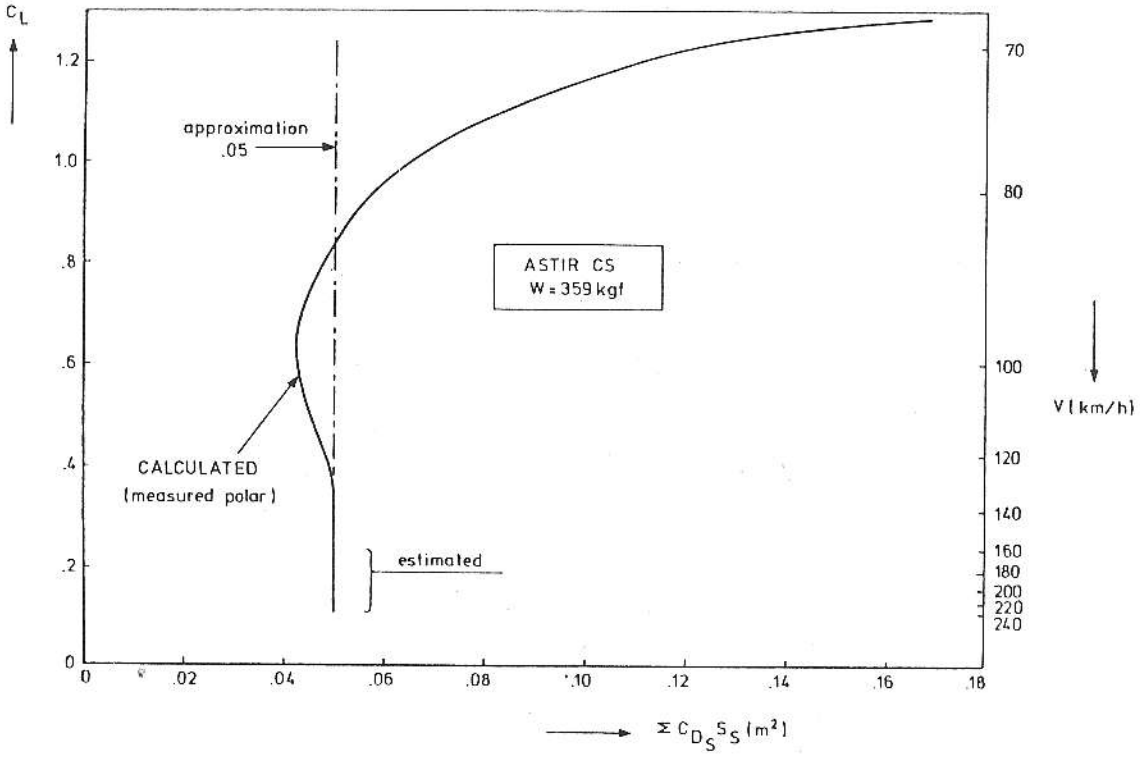

Fig. 7. Parasitic drag area of the Astir CS as function of the lift coefficient.

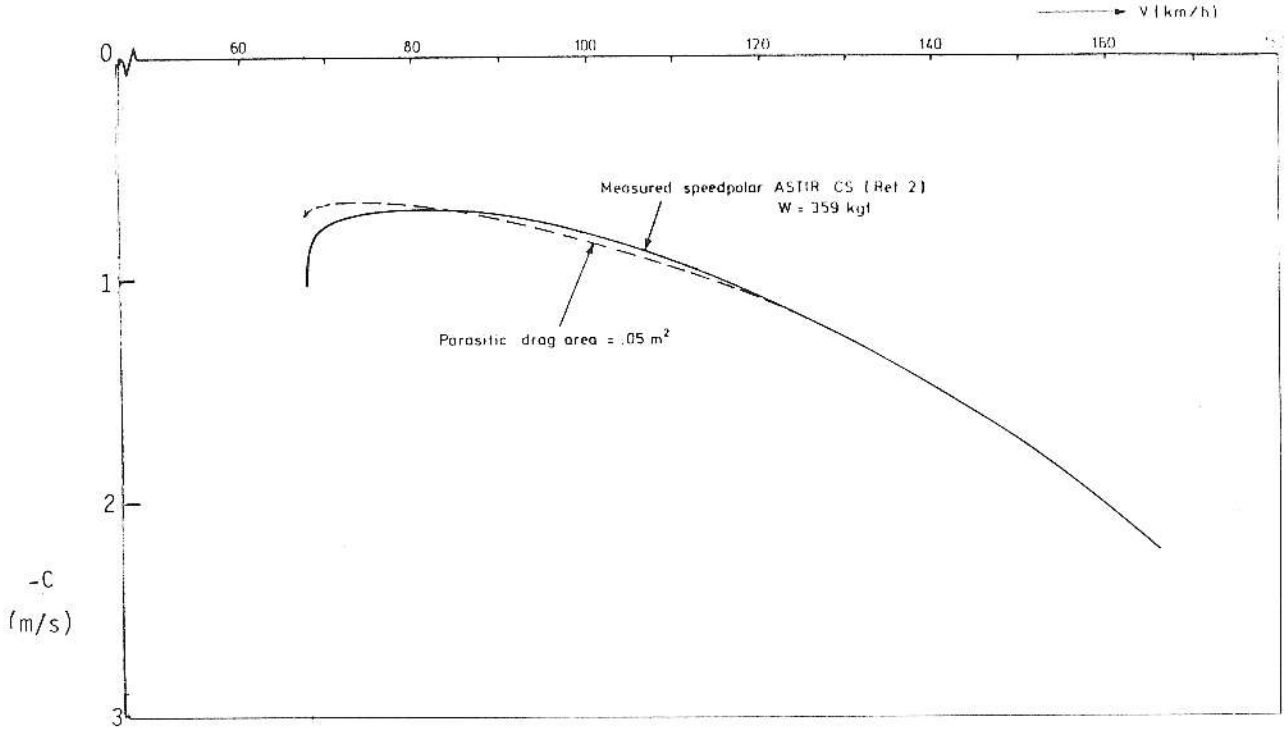

g. 8. Comparison of the Astir CS measured speedpolar and the calculated polar assuming a typical value of the parasitic drag area, fig. 7.

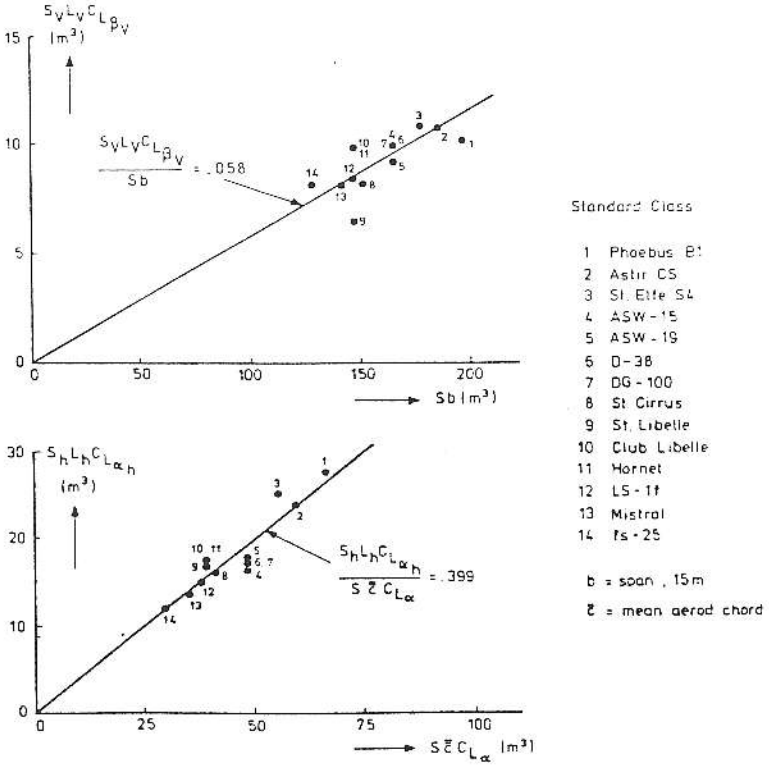

Fig. 9. Horizontal and vertical tail volume at the appropriate reference of 14 high performance Standard Class sailplanes.

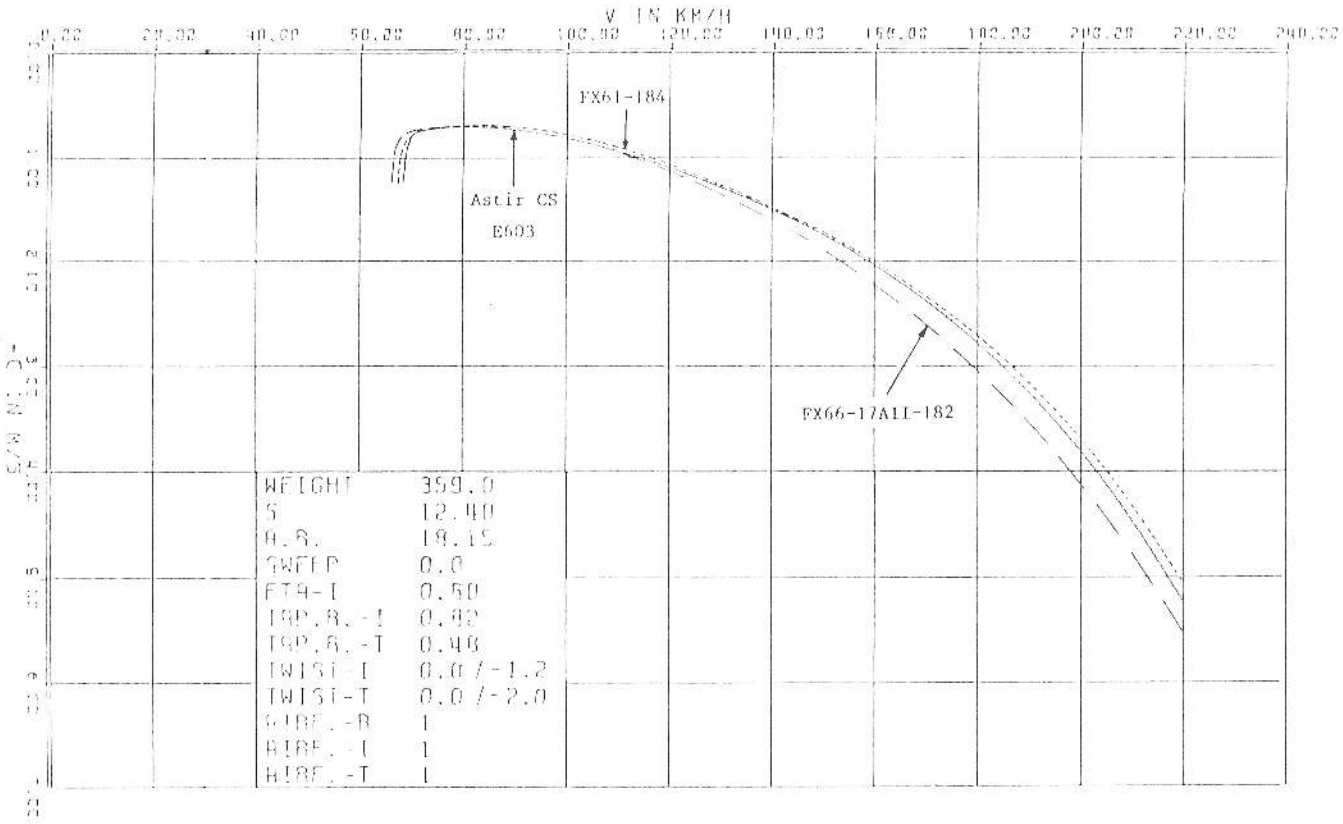

Fig. 10. Calculated speedpolars for the Astir CS with different wing airfoils.

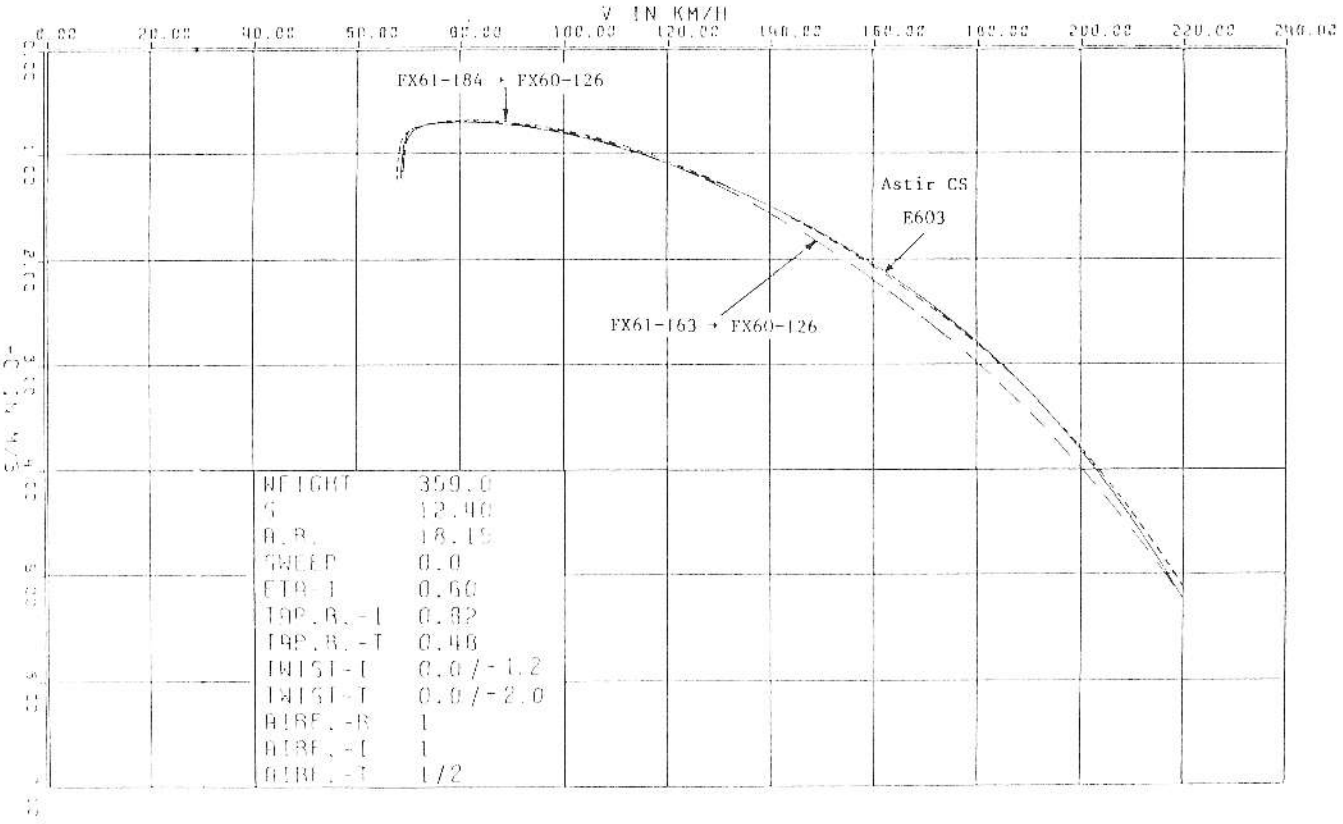

Fig. 11. Calculated speedpolars for the Astir CS with different wing airfoil combinations.

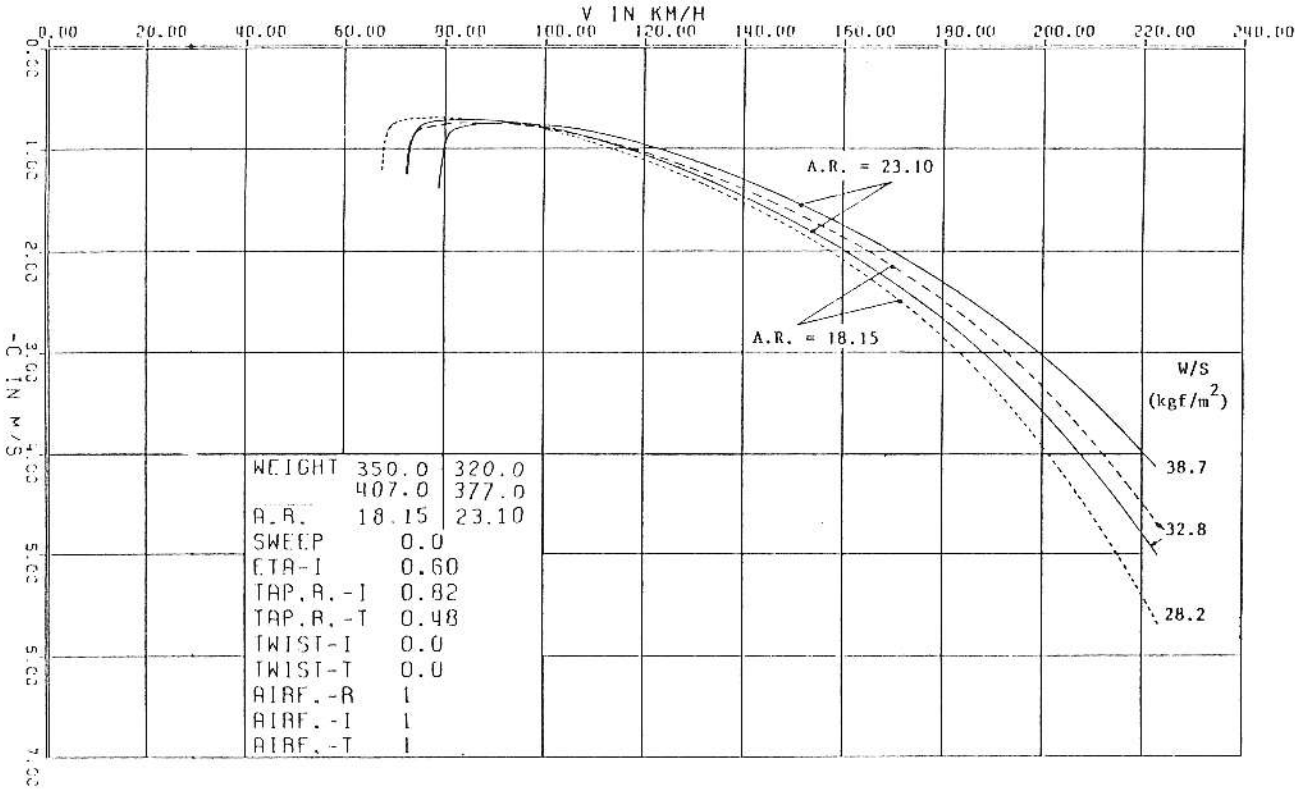

Fig. 12. Alteration of the Astir CS speedpolar when changing aspect ratio and weight.

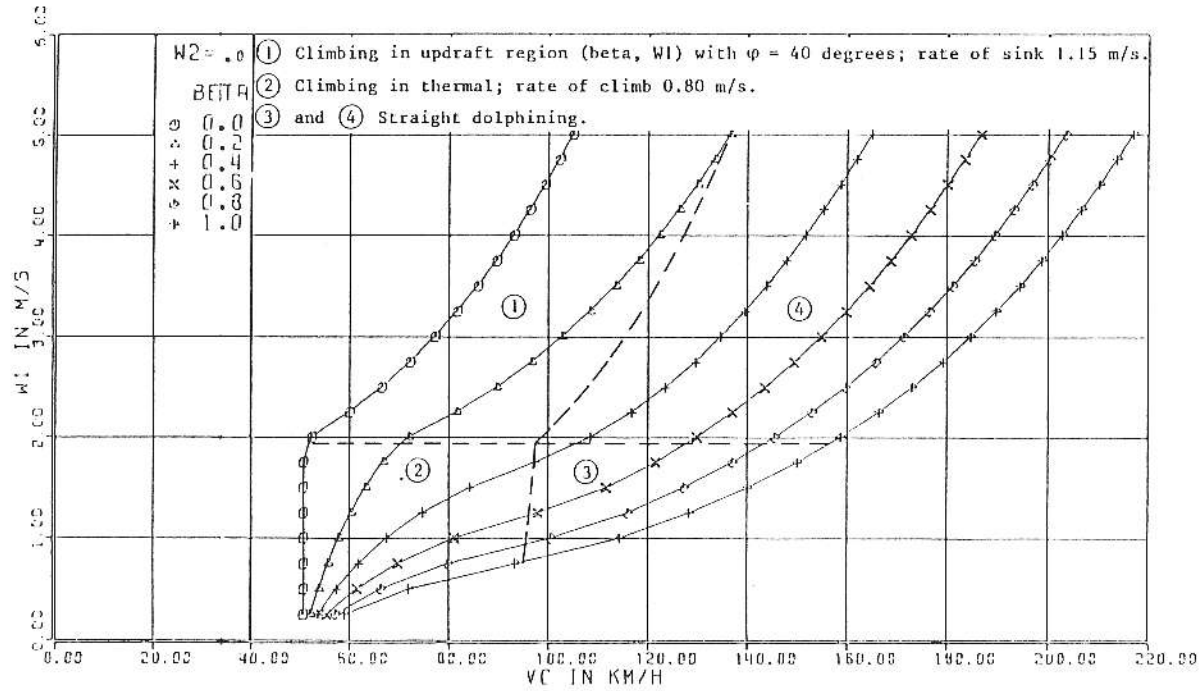

Fig. 13. Cross-country speed of the Astir CS (weight 359 kgf) as a function of meteorological conditions.

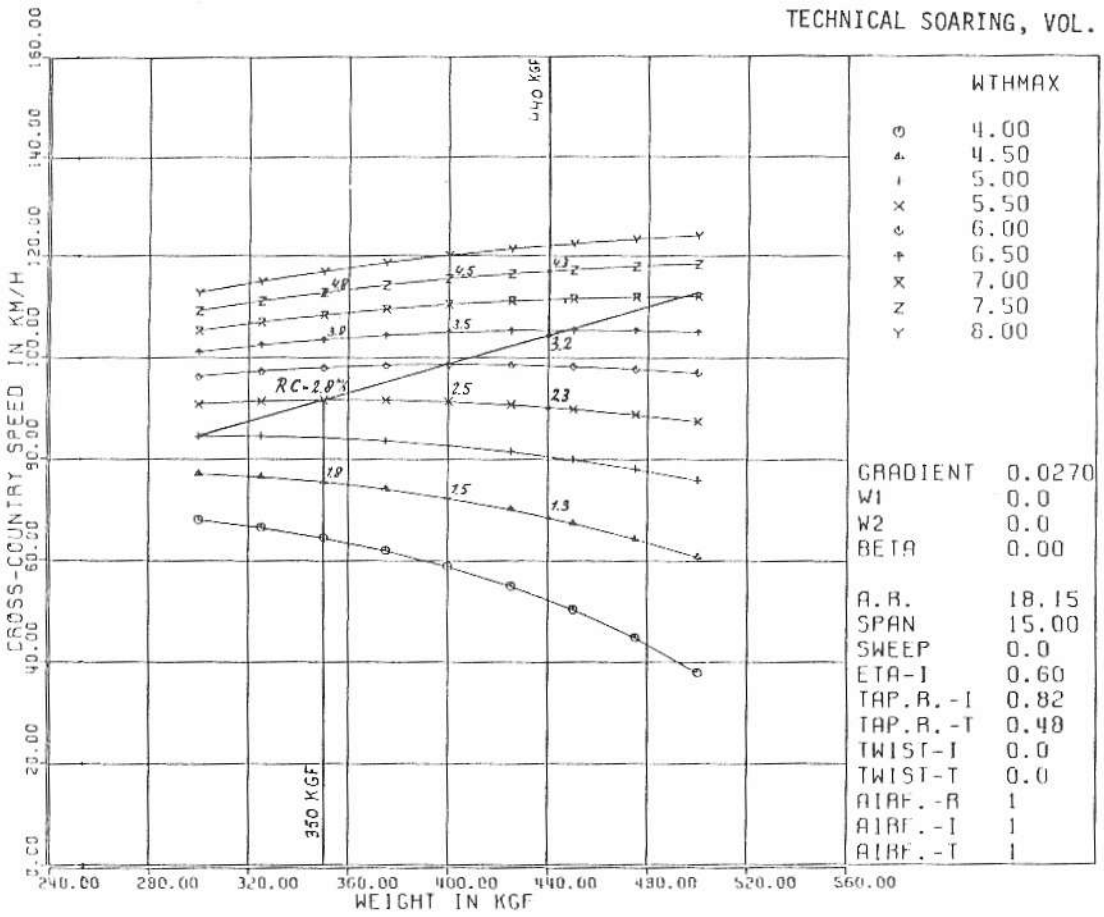

Fig. 14. Cross country speed of the Astir CS as a function of weight and (extrapolated) thermal central strength. Thermals have a linear distribution of vertical velocity (gradient .027 $^{m/s}/_{m}$) in the radius of turn region of interest. Penetration takes place in air which is (on an average) at rest.

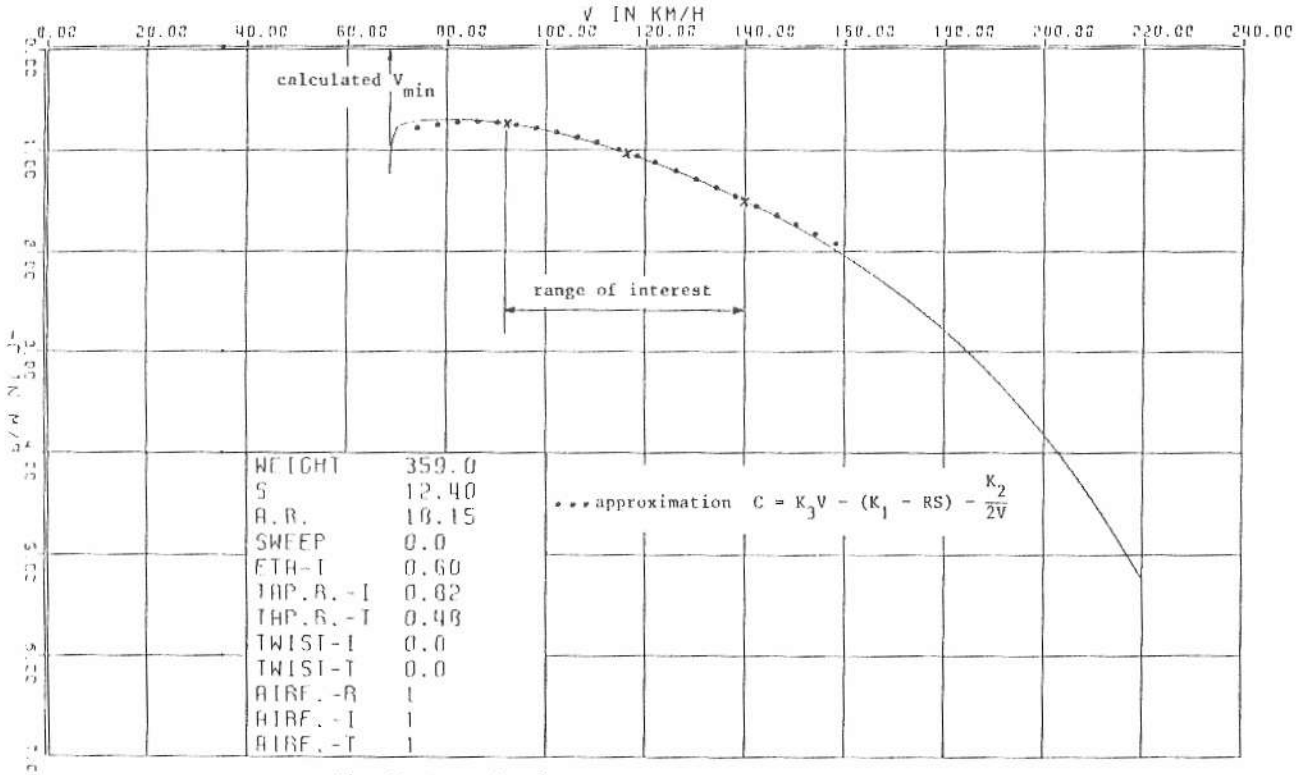

Fig. 1A. Approximation of a relevant part of the Astir CS speedpolar.

FORCE COEFFICIENTS & GLIDING

John McMaster's tutorial on the opposite page is a continuation of those printed in Vol. VI, No. 2. We would appreciate reader reaction to the inclusion of these tutorials in *Technical Soaring*.

FORCE COEFFICIENTS & GLIDING

JH/Hz

Sum of Forces = 0 ⟶ No Acceleration (or change in speed)

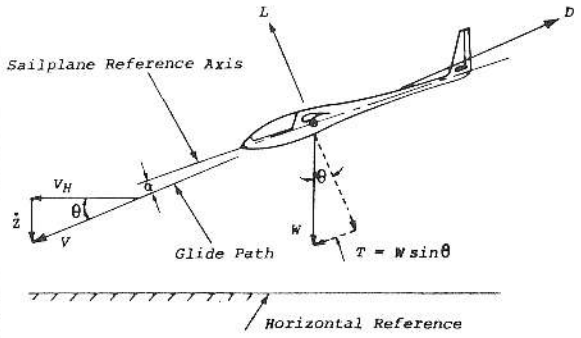

Sum of Forces Parallel to Glide Path = 0 ⟶ $D = W \sin\theta = T$

Sum of Forces Perpendicular to Glide Path = 0 ⟶ $L = W \cos\theta$

Therefore: $\frac{Lift}{Drag} = \frac{L}{D} = \cot\theta = \frac{V_H}{\dot{z}}$

If L/D is greater than about 6, then:

$L \cong W$

$V \cong V_H$

$\frac{L}{D} \cong \frac{V}{\dot{z}} \cong 1/\theta$ (θ measured in Radians)

(1 radian = 57.3°)

L = Lift Force
D = Drag Force
W = Weight
T = Thrust

V = Velocity Along Flight Path
$\dot{z}$ = Sink Rate (Vertical velocity)
θ = Glide Angle
α = Angle of Attack

Pilot's View

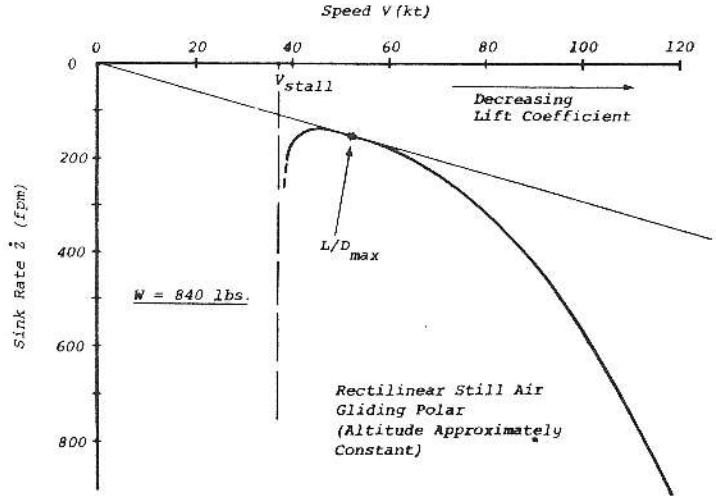

Force Coefficient = $\frac{Force}{q\,S}$

Lift Coefficient = $C_L = \frac{Lift\ Force}{qS}$

Drag Coedficient = $C_D = \frac{Drag\ Force}{qS}$

q = Dynamic Pressure = $1/2\ \rho V^2$

ρ = Air Mass Density

V = Flight Speed

S = Reference Area (Wing Planform Area)

$\frac{Lift}{Drag} = \frac{L}{D} = C_L/C_D$

W = Weight

Engineer's View

Total Drag Coefficient = $C_D = C_{D_W} + C_{D_P} + C_{D_i} + C_{D_t}$ ⟵ Trim Drag

C_{D_W} Parasite Drag; C_{D_P} Profile Drag (Wing); C_{D_i} Induced Drag

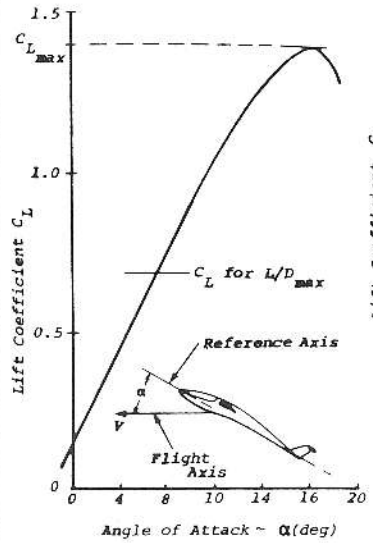

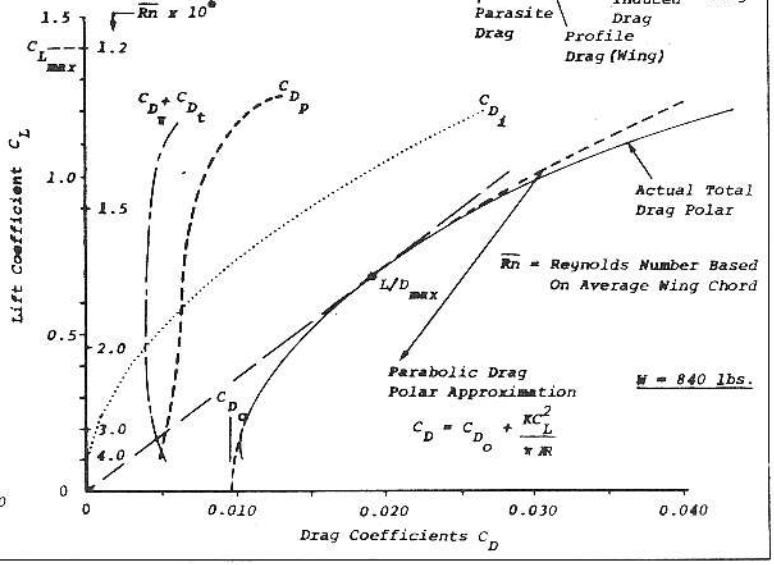

$\overline{Rn}$ = Reynolds Number Based On Average Wing Chord